J. Phys. B: At. Mol. Opt. Phys. 26 (1993) 4169–4181. Printed in the UK

Ionic charge dependence of the zero degree binary encounter peak for partially stripped heavy ions

W Wolff†‡, H E Wolf†‡, J L Shinpaugh†§, J Wang‖, R E Olson‖, P D Fainstein¶, S Lencinas†, U Bechthold‡, R Herrmann† and H Schmidt-Böcking†

† Institut für Kernphysik, Universität Frankfurt, Frankfurt (M), Federal Republic of Germany
‡ Instituto de Fisica, Universidade Federal do Rio de Janeiro, Rio de Janeiro, Brazil
§ Physics Division, Oak Ridge National Laboratory, Oak Ridge, TN, USA
‖ Physics Department, University of Missouri-Rolla, Rolla, MO, USA
¶ Centro Atomico Bariloche and Instituto Balseiro, Bariloche, Argentina

Received 6 July 1993, in final form 13 September 1993

Abstract. We report on the measurements of double differential cross sections, at zero degree, for the production of secondary electrons from the collision of 0.6 MeV amu^{-1} Cu^{5+}, I^{7+}, Au^{11+}, U^{13+}, Cu^{19+}, I^{23+} and Au^{29+} projectiles with H_2 and He. The shapes and positions of the observed binary encounter electron peaks are compared with continuum distorted wave–eikonal initial state (CDW-EIS), impulse approximation and classical trajectory Monte Carlo calculations, as well as with predictions from an adiabatic resonant tunnelling model recently proposed by Fainstein and co-workers. The experimentally observed binary peak positions were found to be essentially determined by the projectile's ionic charge q and to be independent of the projectile's nuclear charge Z_P. Although the experimental conditions correspond to the strong perturbation regime, i.e. $1.0 \leqslant q/V_P \leqslant 5.9$ (V_P being the projectile velocity), the CDW-EIS approach accounts well for the position and shape of the binary peak.

1. Introduction

The production of secondary electrons in collisions involving energetic multiply charged bare ions has been the subject of a series of recent theoretical and experimental investigations, with special emphasis on two-centre electron emission effects (Stolterfoht *et al* 1987, Fainstein *et al* 1991 and references therein, Pedersen *et al* 1991 and references therein, Miraglia and Macek 1991, Fainstein *et al* 1992, Brauner and Macek 1992). Several quantum mechanical approximation schemes, besides the classical trajectory Monte Carlo (CTMC) method, which treats the problem exactly, have been proposed to deal with the active target electron interacting with the projectile and residual target via the Coulomb potential in both initial and final states. Comprehensive compilations and comparisons with available data are given by Miraglia and Macek (1991) and in the topical review of Fainstein *et al* (1991).

The quantum theories (eikonal initial state EIS, continuum distorted wave CDW, impulse approximation IA, strong potential Born approximation SPB and combinations of these like CDW-CDW, CDW-EIS, CDW-IA) all go beyond the first Born approximation by taking into account distortions of the bound state electron wavefunction by the approaching projectile in the initial state and distortions of the continuum state electron wavefunction by both the residual target and the outgoing projectile in the final state. Unlike the FBA they predict binary encounter electron cross sections which scale with the projectile ionic charge q slower than q^2 (Rutherford scaling), binary peaks which become increasingly asymmetric

0953-4075/93/224169+13$07.50

for higher q-values as well as q-dependent energy shifts of the position of the binary peak with respect to the free electron position given by $2V_P^2$ (V_P being the projectile velocity). Similar phenomena are also predicted by CTMC (Reinhold *et al* 1987, Reinhold and Olson 1989). The non-Rutherford scaling behaviour has been termed 'saturation' of the binary encounter (BE) cross section, while the change in position, depending on the direction of the shift, represents a kind of 'binding' or 'antibinding' effect induced by the projectile charge. The EIS and SPB (Brauner and Macek 1992) approximations as well as CTMC and the Bohr–Lindhard (1954) model predict a lowering of the position of the binary peak with respect to the plane wave Born approximation (PWBA) result with increasing projectile charge, while the exact impulse approximation (CDW-IA) suggests a very slight shift towards higher energies (Miraglia and Macek 1991). For the purpose of comparison with experiments it should be noted, however, that the differences between the several theories become significant only for projectile charges $q \geqslant 10$.

Calculations carried out for bare ions are frequently compared to the experimental data of Lee *et al* (1990), who measured zero degree DDCS for 1 to 2 MeV amu^{-1} H^+, C^{6+}, N^7+, O^8+ and F^9+ on H_2 and He, and to the results of Pedersen *et al* (1990, 1991), who reported DDCS at angles from 20° to 160° for 1.0 and 1.8 MeV amu^{-1} H^+, He^{2+}, C^{6+} and O^{8+} on He. In both cases the projectile charges and velocities are well within the range, where all quantum approximation schemes give similar results, so it is desirable to carry out experiments employing ions in higher charge states. Jagutzki *et al* (1991) measured zero degree DDCS for 0.53 MeV amu^{-1} Cu^{5+} and Cu^{15+} and compared their results with a classical CTMC calculation. More experimental results for highly charged ions are only available at considerably higher projectile velocities. Stoltherfoht *et al* (1987) obtained δ-electron cross sections for 25 MeV amu^{-1} Mo^{40+} ions colliding with He. However their data did not extend into the binary encounter region. Schneider *et al* (1989) reported DDCS for 6 MeV amu^{-1} U^{38+} and Th^{38+} projectiles incident on He and Ar, again excluding the binary region of the electron spectra, and more recently (Schneider *et al* 1992) for 3.5 MeV amu^{-1} Fe^{17+} and Fe^{23+} ions, where the binary peak was observed. The experimental results were compared with CTMC, PWBA and CDW-EIS calculations.

Although a variety of ionic species has been employed so far to test the validity of the quantum approximations, the highest values of the Sommerfeld parameter $\kappa = q/V_P$, which gives a measure of the strength of the interaction and of the perturbative nature of the collision (Schneider *et al* 1989, Fainstein *et al* 1991), achieved by Jagutzki *et al* (1991), were $\leqslant 3.3$. The bare ion experiments of Lee *et al* (1990) and Pedersen *et al* (1990, 1991) correspond to even smaller $\kappa \leqslant 1.4$. All approximation schemes include only the first order term of a perturbation series. In the case of CDW-EIS and IA it is the distorted wave series, and in the case of SPB the strong potential Born series. At least for the Born series it is known that it is valid for $\kappa \ll 1$, and it is usually acknowledged that perturbation methods should work in that case. This is the reason for the agreement between all theories for $q \leqslant 10$. First-order distorted wave theories, like CDW-EIS and IA, may be valid for $\kappa \geqslant 1$ because they contain higher orders of the Born series.

In order to test this possibility, we undertook a systematic investigation of the zero degree binary peak employing partially stripped ions with ionic charges q varying from 5 to 29 and with nuclear charges ranging from 29 to 92. With all projectiles having the same velocity equivalent to 0.6 MeV amu^{-1}, q/V_P assumed values between 1.0 an 5.9. The use of clothed ions is dictated by the fact, that bare projectiles of large Z_P atoms are still not feasible in the velocity range studied here. The positions and shapes of the observed binary peaks are compared with quantum mechanical CDW-EIS and IA calculations, with a resonant

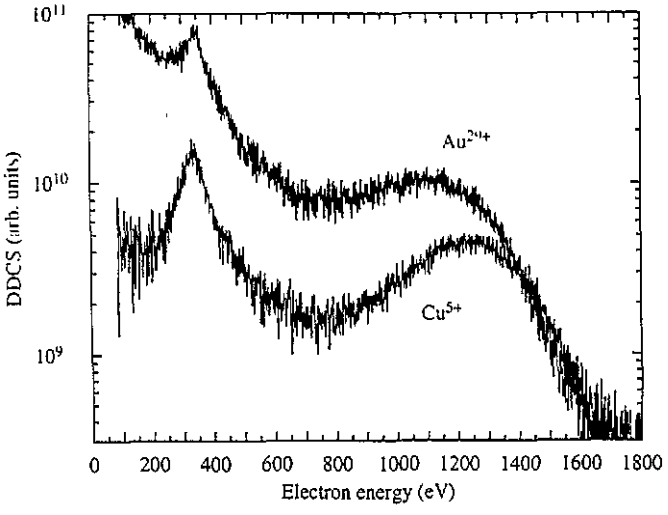

Figure 1. Zero degree DDCS, in arbitrary units, for secondary electron emission from the collision of 0.6 MeV amu^{-1} Cu^{5+} and Au^{29+} with H_2.

tunnelling model proposed by Fainstein *et al* (1992) and with the results of extensive CTMC calculations.

2. Experimental arrangement

The experiments were carried out at the Emperor tandem accelerator of the Max Planck Institut für Kernphysik, Heidelberg. The setup was the same as that used by Wolff *et al* (1992). A detailed description is given by Kelbch (1991) and Kelbch *et al* (1992). The higher charge states were produced by passing the momentum analysed primary low charge beam from the accelerator through a stripper foil and separating the most intense high charge state by a second analysing magnet. The tightly collimated ion beams traversed a differentially pumped gas cell, whose pressure was kept within the 10^{-3} mbar range in order to assure single collision conditions, and were collected by a Faraday cup. Energy spectra of ejected electrons with energies between 100 eV and 2000 eV were recorded at an angle of zero degree with respect to the incident beam with an electrostatic 127° cylinder spectrometer equipped with a channeltron. The accumulated beam charge was used to advance the voltage applied to the plates of the spectrometer in constant steps. Angular and energy resolution of the spectrometer were set to ±1° and 5%, respectively.

3. Results and discussion

We measured double differential cross sections for secondary electron emission, at zero degree, from Cu^{5+}, I^{7+}, Au^{11+}, U^{13+}, Cu^{19+}, I^{23+} and Au^{29+} projectiles with a nominal energy of 0.6 MeV amu^{-1} colliding with H_2 and He. The results obtained for the lowest and highest ionic charge state, Cu^{5+} and Au^{29+}, incident on H_2, are shown in figure 1. The cusp peak at $E_{cusp}=V_p^2/2$ and the binary peak are prominent features of these cross sections. It becomes immediately apparent from the figure, that the Au^{29+} binary peak is located at a considerably lower energy than the Cu^{5+} peak and that it exhibits a strong asymmetry favouring the low energy part of the peak.

Table 1. The ion beams used in this work and the respective beam energies E_P and shifts of the maximum of the binary peak towards lower energies relative to the kinematic binary peak position $4E_{cusp} = 2V_P^2$ for H_2 targets.

Projectile	Cu^{5+}	I^{7+}	Au^{11+}	U^{13+}	Cu^{19+}	I^{23+}	Au^{29+}
E_P (MeV u^{-1})	0.606	0.606	0.580	0.633	0.584	0.582	0.633
Shift (eV)	85±25	95±25	129±25	155±30	192±30	193±35	275±45

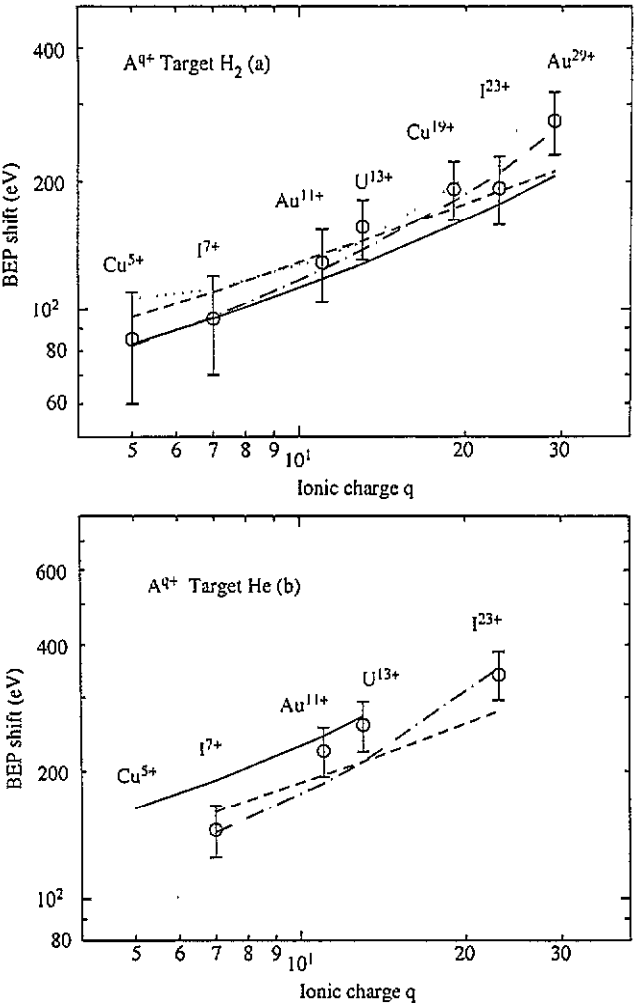

Figure 2. Shift of the binary encounter peak position, towards lower energies, with respect to the free-electron value $2V_P^2$ (eV) as a function of the ionic charge q for H_2 (*a*) and He (*b*) targets. Circle, experimental result; full curve, CDW-EIS result; broken curve, resonant tunnelling model (Fainstein *et al* 1992) with R_c from equation (3); chain curve, resonant tunnelling model with R_c from equation (5); dotted curve, CTMC result (H_2 target only).

In table 1 and figure 2 we present the observed shifts, towards lower energies, of the maximum of the binary peak, with respect to the purely kinematic position $2V_P^2$, as a function of the ionic charge q for H_2 (*a*) and He (*b*) targets. The figure shows the energy shift to be a smooth, monotonically increasing function of q over the entire range ($5 \leqslant q \leqslant 29$) probed in this study. Also included in the figure are calculated energy shifts which will be

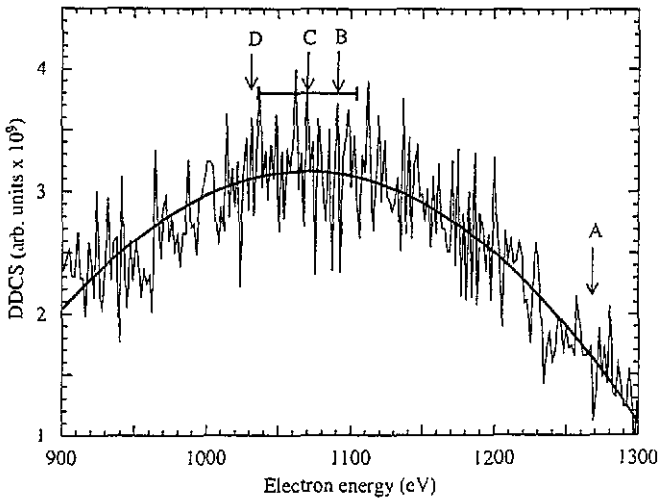

Figure 3. Enlargement of the binary peak from the collision system I^{23+} on H_2. The full curve represent a polynomial of fifth degree fitted to the data in the binary region. Arrows marked A, B and D represent theoretical binary peak positions (free electron value $2V_P^2$, CDW-EIS and CTMC results respectively), while arrow C shows the position of the maximum of the polynomial, chosen to represent the maximum of the experimental binary peak. The horizontal line indicates the uncertainty in the position of that maximum.

discussed below.

The actual beam energies, as determined from the position of the cusp peak, showed slight variations for the several projectiles studied (table 1). These variations from the nominal energy of 0.6 MeV amu^{-1} were contained within the energy interval 0.58 MeV amu^{-1} $\leqslant E_P \leqslant$ 0.63 MeV amu^{-1} and were caused by slightly different accelerator settings for each beam as well as energy loss in the post-stripper foil employed to produce the high charge states. We stress, however, that the small fluctuation of the beam energies is not expected to significantly influence the energy shift of the binary peak, since the shift is obtained as the *relative* difference between the kinematic value $4E_{cusp}$ (using the actual beam energy) and the position of the measured maximum of the binary peak.

The experimental determination of the maximum of the binary encounter peak (BEP) deserves some comments, since the peaks are sometimes very broad. Figure 3 shows the binary peak region for the I^{23+} on H_2 system enlarged and in linear scale. A polynomial of fifth degree was found to fit well the binary region of the DDCS. The position of the maximum of the binary peak was then derived from the maximum of the polynomial. Upper and lower boundaries for the position of the maximum were established by fixing limits beyond which the maximum certainly is not located. The experimental BE peak position (an arrow marked with the letter C) as well as the associated uncertainty are indicated in figure 3. For the sake of comparison the purely kinematic position given by $4E_{cusp}$ as well as binary peak positions predicted by CDW-EIS and CTMC calculations (see below) are also included in figure 3 (arrows marked A, B and D respectively).

Before we proceed to compare the experimental results with predictions from several model calculations, a few observations are in order. Objections may be raised as to the validity of a comparison between the present experimental data and a CDW-EIS calculation, since we are dealing with screened ions, and the distorted wave calculations in the exit channel can so far only be performed for bare ions. Therefore the following argument should be considered. The electron wavefunction used in the CDW-EIS approach (Crothers

and McCann 1983, Fainstein *et al* 1988, 1989, 1992) is distorted by the long range Coulomb potential of the approaching projectile in the initial state and by the long range Coulomb potentials of both the outgoing projectile and residual target in the final state. So it is the ionic charge q of the projectile which is responsible for the additional phase, in the EIS approximation, to the initial bound state electronic wavefunction, and for one of the two Coulomb factors in the CDW approximation to the final continuum state wavefunction.

With regard to the position of the binary peak due to the initial and final state distortions, we note that the energy shift of the binary peak with respect to the free electron value $2V_P^2$ is determined in part by the electron elastic scattering cross section near 180° in the projectile rest frame (Wang *et al* 1991). Although the elastic scattering cross section for a screened ion is much different from the Rutherford cross section for the same ionic charges, the shape near 180° ($\sim$ 170°–180°) is very flat in both cases (see figure 5). This similarity suggests that as far as the peak position at 0° is concerned the distortion may be adequately represented by a pure Coulombic ion at this angle.

In the framework of the resonant tunnelling model the energy shift of the binary peak with respect to the free electron value $2V_P^2$ is determined by how deep the initially bound electron penetrates into the projectile field before being stripped off (or released from) the target (Bohr and Lindhard 1954, Fainstein *et al* 1992). The ionic charges of the projectiles used in the present work are all much larger than unity, which is the charge which binds the electron in the hydrogen atom, and the electronic charge distributions of the ions themselves have radii considerably smaller than 1 au. These two facts combined suggest that the target electron might be ionized at a distance from the projectile where it is still far outside the *projectile's electronic charge distribution.*

The arguments presented in the preceding two paragraphs encouraged us to apply the bare-ion CDW-EIS approach to describe the position and shape of the binary peak of clothed projectiles. However a word of caution is in order, too. It is well known from recent experimental and theoretical work performed on clothed ions (Kelbch *et al* 1989, Richard *et al* 1990, Reinhold *et al* 1991, Schultz and Olson 1991, Hagmann *et al* 1992, Wolff *et al* 1992) that the shape and magnitude of the binary peak are strongly affected by quantum interference structures in the scattering of target electrons by the screened projectile field. For that reason it is not to be expected that the scaling behaviour of the clothed ion binary peak will be correctly described by CDW-EIS. In addition, if there is a pronounced diffraction minimum close to 180° (in the projectile frame of reference) in the cross section for the elastic scattering of electrons in the screened projectile field, it might affect the shape of the binary peak at zero degree, so the CDW-EIS approach would not be expected to account for the BEP shape under these circumstances.

In figure 4 we present the experimental DDCS for I^{7+} and I^{23+} incident on H_2 and He. The iodine ions were chosen for this comparison, because it is known from previous work (Wolff *et al* 1992) that there is no diffraction minimum close to 180° in the calculated electron elastic scattering cross section for the field of these projectiles. These cross sections, together with the Rutherford cross sections for $q = 7$ and 23, are reproduced from the work of Wolff *et al* in figure 5, which refers to the projectile frame of reference. Both screened ion cross sections exhibit broad diffraction maxima at 180°, which are responsible for an enhancement of the 0° BE cross sections over the $q = 7$ and $q = 23$ Rutherford values, while the nearest diffraction minima are located around 140°. The enhancement factors assume values of 150 and 17 for I^{7+} and I^{23+}, respectively. The different enhancement factors lead to electron scattering cross sections, which have similar values, at 180°, for both projectiles (3.0 au and 3.7 au respectively for I^{7+} and I^{23+}).

In order to obtain a more quantitative understanding of the influence of quantum

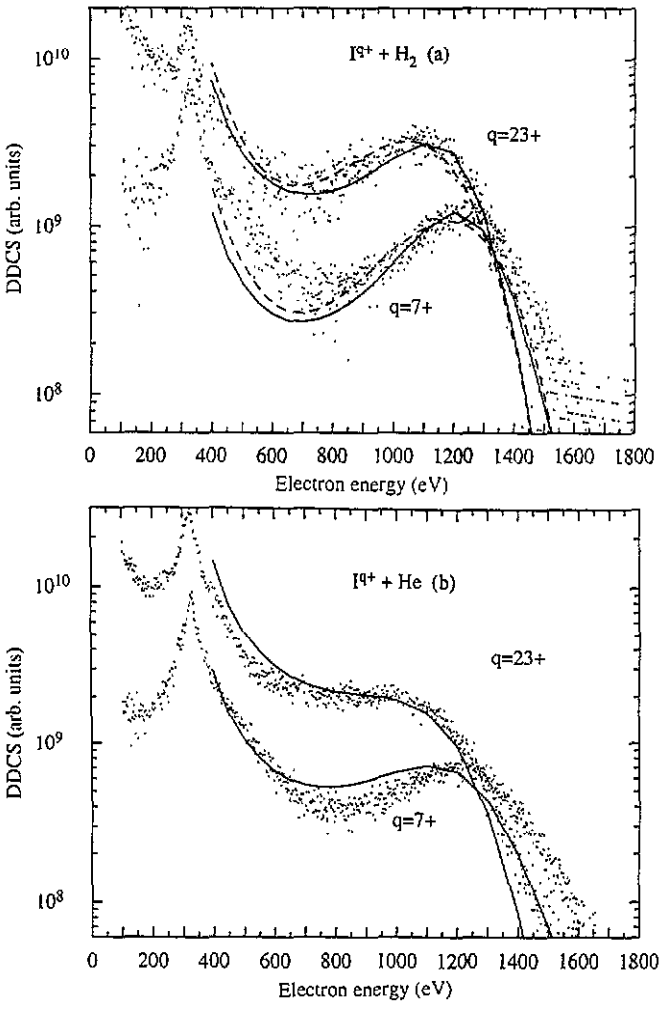

Figure 4. Zero degree DDCS, in arbitrary units, for secondary electron emission from the collision of 0.6 MeV amu^{-1} I^{7+} and I^{23+} with H_2 (*a*) and He (*b*), compared with the results of CDW-EIS and CTMC calculations carried out for bare ions with charges 7+ and 23+. Full curve, CDW-EIS; broken curve, CTMC (H_2 target only). The theoretical curves were normalized separately to the respective data.

diffraction effects on the shape of the 0° binary peak, an impulse approximation calculation was performed for I^{7+} and I^{23+} incident on H_2 using a method adapted from the one previously employed by Wang *et al* (1991) for treating electron loss. The initial state is represented by an IA wavefunction (equation (3) of the work of Wang *et al*) similar to that given in the paper of Miraglia and Macek (1991) (their equation (2.5)), with the difference, that instead of Coulomb electron wavefunctions, whose form is known analytically, numerically developed wavefunctions representing continuum states of the electron in the non-Coulomb field of the projectile were used. Because of the great numerical difficulties encountered when using this type of wavefunction, the final state electron wavefunction was represented by a plane wave. A two-centre Coulomb wavefunction, like that of equation (2.1) of Miraglia and Macek, would not have been the appropriate choice for the final state, because of the non-Coulomb nature of the projectile field. Since

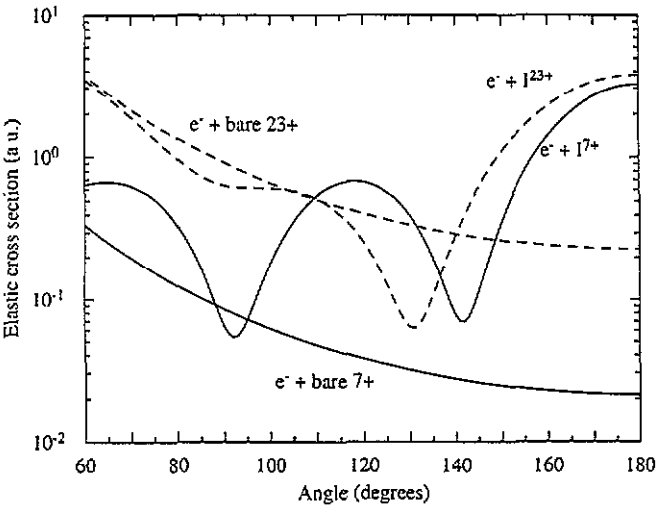

Figure 5. Model cross sections for the elastic scattering of 327 eV (equivalent to 0.6 MeV amu^{-1}) electrons in the screened potentials of I^{7+} and I^{23+} from Wolff *et al* (1992). Rutherford cross sections for Coulomb potentials with charges 7+ and 23+ are also given. The figure refers to the projectile frame of reference.

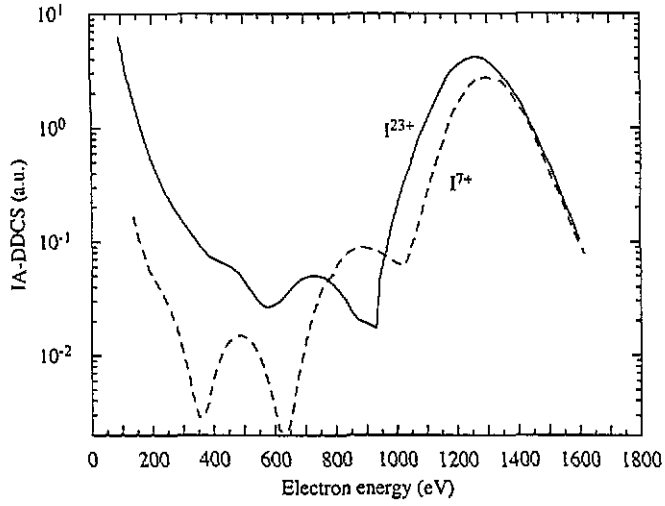

Figure 6. DDCS for electron emission, at 0°, calculated in impulse approximation for I^{7+} and I^{23+} incident on H. The screened nature of the projectiles has been taken into account, and is responsible for the marked interference structures. No final state interaction was included in this calculation.

final state interactions are therefore excluded from the present IA calculation, certain features of the observed DDCS are not reproduced, as will be shown below.

The results of the IA calculation are shown in figure 6. While quantum interference effects clearly manifest themselves in the form of alternating minima and maxima in the calculated DDCS, at this extreme forward angle the binary peaks are not affected by them. A small energy shift of 35 eV in the binary peak is noted between I^{7+} and I^{23+}, whose maxima are located at 1300 eV and 1265 eV, respectively. The binary peaks have almost equal amplitudes, a fact already expected from the preceding discussion of the elastic electron

scattering cross sections, and are symmetric in shape. Since no final state interactions have been taken into account, no cusp peaks are present in these DDCS. It is obvious from the figure, that the shapes and positions of the experimentally observed binary peaks for I^{7+} and I^{23+} projectiles incident on H_2 (figure 4(*a*)), which exhibit a pronounced low energy asymmetry and a considerable energy shift between I^{7+} and I^{23+}, are not reproduced by this IA calculation, probably for the same reason responsible for the lack of a cusp peak, i.e. the non-inclusion of the interaction between the ejected electron and the outgoing projectile, as well as the polarization of the initial state.

Calculations with CDW-EIS and CTMC were performed for bare projectiles with charges q of 7 and 23, and the results are shown in figure 4. The CDW-EIS cross sections, which exhibit a $q = 23$ over $q = 7$ BEP amplitude ratio of 8.3, and CTMC cross sections were normalized separately to the maxima of the experimental binary peaks, whose amplitude ratio is 2.6. In the case of the H_2 target (figure 4(*a*)) the calculations account reasonably well for the shapes and positions of the binary peaks, including their strong asymmetry, but slightly underestimate the high energy part of spectra. The intermediate energy region, i.e. the region between the cusp and BE peaks, of the I^{7+} DDCS is also slightly underestimated by both theories, presumably because it contains projectile electrons scattered by the target and promoted into the continuum (electron loss to continuum, or ELC). ELC electrons are less likely to be produced in collisions of I^{23+}, since in this latter case the projectile electrons are more tightly bound. On the theory side, CDW-EIS and CTMC results for I^{7+} agree extremely well with each other. The agreement is less satisfactory in the case of I^{23+}, notably in the peak positions. The difference is due to the large perturbation in the latter case.

The same comparison between CDW-EIS and experiment is carried out in figure 4(*b*) for a He target. Again CDW-EIS reproduces well the general tendency observed when going from low to high charge states, but now the discrepancy for the high energy part of the I^{7+} BEP is more pronounced, with the calculated peak being located at a lower energy with respect to the experimental one. Surprisingly CDW-EIS predicts more intermediate energy electrons, i.e. electrons filling the 'valley' between the BE and cusp peaks, than seen in the experiment. The opposite behaviour would be expected, since the intermediate energy region of the experimental DDCS may always be 'contaminated' by an unknown amount of ELC electrons, which in addition are expected to be more numerous for the He than the H_2 target.

In figure 2 we compare the observed BEP energy shifts with CDW-EIS and CTMC calculations for a bare projectile with ionic charge q as well as with the predictions of a resonant tunnelling model proposed by Fainstein *et al* (1992). In this model the velocity v_{T-e} of the ejected BE electron in the laboratory frame is given by (all quantities appearing in the equations are in atomic units):

$$v_{T-e} = V_P \cos\theta_L + (V_P^2 \cos^2\theta_L + v_{P-e}^2 - V_P^2)^{1/2} \tag{1}$$

$$v_{P-e}^2 = V_P^2 + 2\epsilon_i - 2\frac{Z_P}{R_c} \tag{2}$$

where V_P is the projectile velocity, θ_L the angle of observation, v_{P-e} the electron velocity in the projectile frame, ϵ_i the electron binding energy and R_c the effective internuclear distance at which the electron is released from the target. In the present work two different sets of R_c values are used. One set is obtained from the implicit equation given by Fainstein *et al* (1992)

$$U_p(R_c) - U_p(R_c - a_i) \simeq |\epsilon_i| \tag{3}$$

$$a_i = \frac{3}{2Z_T} \tag{4}$$

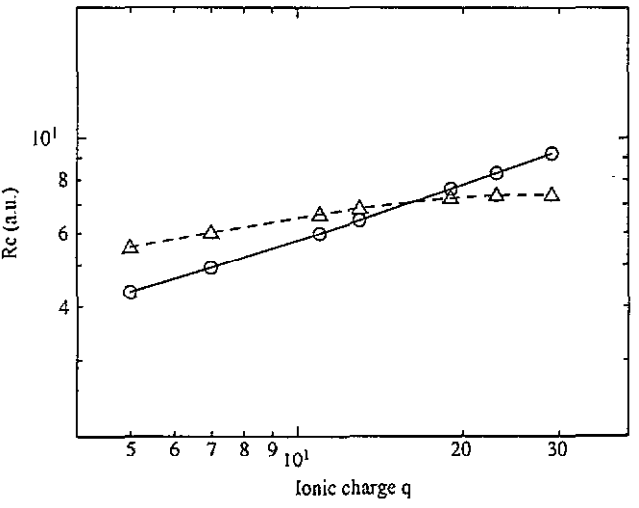

Figure 7. Internuclear distances R_c used in calculating the energy shifts of figure 2 from the resonant tunnel model plotted against ionic charge q for the hydrogen target. Circle, R_c calculated from equation (3); triangle, R_c calculated from equation (5).

with U_p being the projectile potential and a_i the target electron orbital radius. In the present work a screened potential (Green–Garvey potential, Garvey *et al* 1975) as well as a Coulomb potential for an ionic charge q were chosen for U_p and equation (3) solved numerically. The two choices of potential yielded practically identical results. Another set of R_c values was obtained from the work of Olson and Salop (1976), who studied electron transfer between multicharged ions and neutral atoms. In that work the charge exchange cross section is given by $Q = \pi R_c^2$, where R_c is some critical projectile–target distance within which the transfer probability is unity. Values for R_c were obtained by numerically solving their equation (10), which reads in modified notation:

$$R_c^2 \exp[-2.628\alpha R_c/q^{1/2}] = 2.864 \times 10^{-4} q(q-1)V_P \tag{5}$$

$$\alpha = [I_t(\text{eV})/13.6]^{1/2} \tag{6}$$

where q is the projectile ionic charge, and I_t the ionization potential of the target atom. Both sets of R_c values are given as a function of q for the case of a hydrogen target in figure 7.

As can be seen from figure 2(a) the shift of the binary peak, towards lower energies, increases smoothly with the ionic charge q, despite the fact that we are comparing, in the same figure, clothed ions of strongly varying degrees of screening. This empirical finding supports the aforementioned view, that the Rutherford and the screened elastic scattering cross sections are both smooth near 180°. Generally speaking both the CDW-EIS and CTMC calculations, carried out for bare ions, describe fairly well the experimentally observed binary peak shifts. In particular the CDW-EIS results reproduce well the energy shifts observed for lower charge states, but do not quite accompany the tendency of an increasing energy shift observed for the higher charge states, although the theoretical results always lie within the experimental uncertainty (with the exception of Au^{29+}). This behaviour of CDW-EIS is not unexpected, since the higher charge states correspond to values of $q/V_P \gg 1$, where a first order perturbation approach may become inadequate. With exception of the I^{23+} case, the CTMC results also fall inside the experimental error bars, and show improving

agreement with the data as the ionic charge increases. In fact it appears from figure 2(*a*) that the CDW-EIS and CTMC results mark a lower and upper limit respectively for the binary peak shift, while the data are located somewhere in between. The resonant tunnelling model, when employing R_c values given by equation (3), overestimates the energy shift for lower q-values, while underestimating it for higher q-values. Very good agreement with the data over the entire range of q-values, on the other hand, is achieved by the resonant tunnelling model when employing the internuclear distances from Olson and Salop (1976, equation (5)).

Figure 7 shows that the internuclear distance R_c at which, according to the tunnelling model, the electron is effectively released from the target, assumes values between 4 and 10 au. These large values are indicative of the large distortion exerted on the target system by the highly charged projectile ion and underscores the importance of incorporating distortion effects into theoretical models.

The experimental results obtained for the He target (figures 2(*b*) and 4(*b*)) are not so well described by CDW-EIS, which predicts too large an energy shift of the binary peak position for low q-values. Towards higher charge states an improvement is noted, but no comparison could be carried out for $q = 23$, since CDW-EIS did not yield a well defined binary peak for that high charge state because of the broad Compton profile of He. For the same reason $q = 29$ did not yield proper peaks neither in experiment nor in theory, but only shoulders with no detectable maximum. The resonant tunnelling model proves more successful in predicting the binary peak shifts, and again the results obtained with the R_c values taken from Olson and Salop produce the better agreement with the data.

4. Conclusions

We have presented a systematic study of the position and shape of the binary encounter peak for ionic charges from 5+ to 29+ in the intermediate velocity regime (0.6 MeV amu^{-1}) corresponding to values of the Sommerfeld parameter q/V_P between 1.0 and 5.9. The ionic species employed possessed strongly varying degrees of screening, from Cu^{19+} to U^{13+}. It was found that the shift of the position of the binary peak with respect to the free electron value $2V_P^2$ depended only on the ionic charge of the projectile, and not on its nuclear charge. The resonant tunnelling model from Fainstein *et al* (1992) gave an excellent quantitative description of these shifts over the entire charge range studied. A CDW-EIS calculation performed for bare ions with charges 7+ and 23+ accounted very well for the shapes of the binary peaks produced from the screened ions I^{7+} and I^{23+} colliding with H_2. While the binary peak positions calculated with CDW-EIS showed good agreement for the lower charge states, but somewhat underestimated the shifts observed for the highest ionic charges, the opposite trend is observed in the CTMC results, with the exception of the 23+ charge state. We conclude that screening effects do not seem to be important for the position of the binary peak at zero degree observation angle, because of the flatness of the elastic electron cross section near 180°. Although of course they strongly affect its magnitude. The CDW-EIS approach, despite being a first-order perturbative theory, accounts well for the position and shape of the binary peak even in the strong perturbative regime of $q/V_P \gg 1$. The somewhat unexpected mediocre performance of CDW-EIS in predicting the binary peak positions for low charge states in the case of a He target is at present not understood. Conceivably the small ionic charge and strong screening of the I^{7+} ion, combined with a larger binding energy of the electron in the He atom, may limit the bare ion approach in that particular case.

Acknowledgments

We wish to thank the Emperor tandem accelerator laboratory of the Max Planck Institut für Kernphysik Heidelberg for the innumerous hours of beam time they provided, and for the competent help and advice of Dr R Repnow in preparing particularly difficult beams. Three of the authors (WW, HEW and JLS) would like to express their gratitude for the hospitality and friendship received and for fruitful discussions during their stay at the Institut für Kernphysik Frankfurt. HEW and JLS acknowledge financial support received during the course of this work: HEW to the Conselho Nacional de Desenvolvimento Cientifico e Tecnologico (Brazil) for a post-doctoral grant and JLS to the Fullbright Commission (USA) and Humboldt Foundation (Germany) for research fellowships. Financial support from DFG, BMFT and the Office of Fusion Energy, US Department of Energy is also acknowledged.

References

Bohr N and Lindhard J 1954 *K. Dansk. Vidensk. Selsk. Mat.-Fys. Meddr.* **28** 1

Brauner M and Macek J H 1992 *Phys. Rev.* A **46** 2519

Crothers D S F and McCann J F 1983 *J. Phys. B: At. Mol. Phys.*. **16** 3229

Fainstein P D, Ponce V H and Rivarola R D 1988 *J. Phys. B: At. Mol. Opt. Phys.* **21** 287

—— 1989 *J. Phys. B: At. Mol. Opt. Phys.* **22** 1207

—— 1991 *J. Phys. B: At. Mol. Opt. Phys.* **24** 3091

—— 1992 *Phys. Rev.* A **45** 6417

Garvey R H, Jackmann C H and Green A E S 1975 *Phys. Rev.* A **12** 1144

Hagmann S, Wolff W, Shinpaugh J L, Wolf H E, Olson R E, Bhalla C P, Shingal R, Kelbch C, Herrmann R, Jagutzki O, Dvrner R, Koch R, Euler J, Ramm U, Lencinas S, Dangendorf V, Unverzagt M, Mann R, Mokler P, Ullrich J, Schmidt-Böcking H and Cocke C L 1992 *J. Phys. B: At. Mol. Opt. Phys.* **25** L287

Jagutzki O, Hagmann S, Schmidt-Böcking H, Olson R E, Schultz D R, Dörner R, Koch R, Skutlartz A, Gonzalez A, Quinteros T B, Kelbch C and Richard P 1991 *J. Phys. B: At. Mol. Opt. Phys.* **24** 2579

Kelbch C, Hagmann S, Kelbch S, Mann R, Olson R E, Schmidt S and Schmidt-Böcking H 1989 *Phys. Lett.* **139A** 304

Kelbch C 1991 *GSI Report* GSI-91-12 April

Kelbch C, Koch R, Hagmann S, Ullmann K, Schmidt-Böcking H, Reinhold C O, Schultz D R, Olson R E and Kraft G 1992 *Z. Phys.* D **22** 713

Lee D H, Richard P, Zouros T J M, Sanders J M, Shinpaugh J L and Hidmi H 1990 *Phys. Rev.* A **41** 4816

Miraglia J E and Macek J 1991 *Phys. Rev.* A **43** 5919

Olson R E and Salop A 1976 *Phys. Rev.* A **14** 579

Pedersen J O P, Hvelplund P, Petersen A G and Fainstein P D 1990 *J. Phys. B: At. Mol. Opt. Phys.* **23** L597

—— 1991 *J. Phys. B: At. Mol. Opt. Phys.* **24** 4001

Reinhold C O, Falcon C and Miraglia J E 1987 *J. Phys. B: At. Mol. Phys.* **20** 3737

Reinhold C O and Olson R E 1989 *Phys. Rev.* A **39** 3861

Reinhold C O, Schultz D R, Olson R E, Kelbch C, Koch R and Schmidt-Böcking H 1991 *Phys. Rev. Lett.* **66** 1842

Richard P, Lee D H, Zouros T J M, Sanders J M and Shinpaugh J L 1990 *J. Phys. B: At. Mol. Opt. Phys.* **23** L213

Schneider D, DeWitt D, Schlachter A S, Olson R E, Graham W G, Mowat J R, DuBois R D, Loyd D H, Montemayor V and Schiwietz G 1989 *Phys. Rev.* A **40** 2971

Schultz D R and Olson R E 1991 *J. Phys. B: At. Mol. Opt. Phys.* **24** 3409

Stolterfoht N, Schneider D, Tanis J, Altevogt H, Salin A, Fainstein P D, Rivarola R, Grandin J P, Scheurer J N, Andriamonje S, Bertault D and Chemin J F 1987 *Europhys. Lett.* **4** 899

Wang J, Reinhold C O and Burgdörfer J 1991 *Phys. Rev.* A **44** 7243

Wolff W, Shinpaugh J L, Wolf H E, Olson R E, Wang J, Lencinas S, Piscevic D, Herrmann R and Schmidt-Böcking H 1992 *J. Phys. B: At. Mol. Opt. Phys.* **25** 3683